

Microvascular abnormalities in sickle cell disease: a computer-assisted intravital microscopy study

Anthony T. W. Cheung, Peter C. Y. Chen, Edward C. Larkin, Patricia L. Duong, Sahana Ramanujam, Fern Tablin, and Ted Wun

The conjunctival microcirculation of 18 homozygous sickle cell disease (SCD) patients during steady-state, painful crisis, and postcrisis conditions was recorded on high-resolution videotapes using intravital microscopy. Selected videotape sequences were subsequently coded, frame-captured, studied, and blindly analyzed using computer-assisted image analysis protocols. At steady-state (baseline), all SCD patients exhibited some of the following morphometric abnormalities: abnormal vessel diameter, comma signs, blood sludging, boxcar blood flow phenomenon, distended vessels, damaged vessels, hemosiderin deposits, vessel tortuosity, and micro-

aneurysms. There was a decrease in vascularity (diminished presence of conjunctival vessels) in SCD patients compared with non-SCD controls, giving the bulbar conjunctiva a “blanched” avascular appearance in most but not all SCD patients during steady-state. Averaged steady-state red cell velocity in SCD patients was slower than in non-SCD controls. During painful crisis, a further decrease in vascularity (caused by flow stoppage in small vessels) and a $36.7\% \pm 5.2\%$ decrease in large vessel (mostly venular) diameter resulted. In addition, the conjunctival red cell velocities either slowed significantly ($6.6\% \pm 13.1\%$; $P < .01$) or were reduced to a trickle (unmeasurable) during crisis.

The microvascular changes observed during crisis were transient and reverted to steady-state baseline after resolution of crisis. When combined, intravital microscopy and computer-assisted image analysis (computer-assisted intravital microscopy) represent the availability of a noninvasive tool to quantify microvascular abnormalities in vascular diseases, including sickle cell disease. The ability to identify and relocate the same conjunctival vessels for longitudinal studies uniquely underscores the applicability of this quantitative real-time technology. (Blood. 2002;99:3999-4005)

© 2002 by The American Society of Hematology

Introduction

Sickle cell disease (SCD) is a compendium of genetic diseases that primarily includes homozygous sickle cell anemia (HbSS), compound heterozygous combinations of HbS and β thalassemia (HbS-thal), and heterozygous (HbS-HbC) disease (HbSC).^{1,2} A single amino acid substitution (Glu to Val) in the β -globin chain of hemoglobin in SCD patients leads to myriad clinical effects and complications.^{1,3} With much improved treatment for infections and the availability of blood transfusion products for hypoplastic crisis, the life expectancy of patients with HbSS has improved considerably since 1960.^{4,5} Nonetheless, SCD patients have significantly decreased survival rates when compared with age-, sex-, and ethnic-matched control groups.^{2,5} Vascular pathology (vasculopathy) underlies most of the complications and accounts for much of the morbidity and mortality.^{3,5,6} However, real-time studies characterizing the in vivo microvascular abnormalities of SCD patients have rarely been conducted.⁷⁻⁹

Sludging of blood and the presence of comma signs in the vessels of the bulbar conjunctiva in SCD patients were first noted decades ago by Knisely et al¹⁰ and Paton,^{11,12} respectively. Blood sludging and comma signs are caused by stagnation of blood flow in conjunctival vessels resulting in extremely slow or no blood movement; sludging can be seen

when mid-sized to large-sized vessels are compacted with red cells (“S” in Figures 1B-D and 2), while comma signs are seen as short columns of stationary red cells in small obstructed vessels (“CS1” and “CS2” in Figure 2, for the 2 unique shapes of comma signs observed). When blood flow in the small conjunctival vessels (mostly in arterioles and sometimes small venules) is sluggish or intermittent, the boxcar blood flow phenomenon—so called because of its unique railway boxcar aerial appearance—results (“BC” in Figures 1B and 2). Pioneering SCD investigators^{8,9,13-19} have used the conjunctival microcirculation in their research, speculating that the abnormalities were of significance not only because they could be detected but that they might reflect functionally and morphologically more deleterious or pathological microvascular events in the jeopardized tissues. These historical studies were based on slit-lamp biomicroscopy via 35-mm photography, and the results were mostly descriptive and rarely quantified.⁸⁻¹⁹

It is normally not possible to directly study real-time microvascular abnormalities leading to soft tissue end organ damage in SCD patients. However, the readily accessible microvascular bed of the bulbar conjunctiva offers an excellent noninvasive site to extrapolate the in vivo microvascular condition at the soft tissue end organ level. We have used the conjunctival microcirculation in this study

From the Department of Medical Pathology, University of California (UC) Davis School of Medicine, Davis, CA; Department of Bioengineering, UC San Diego, La Jolla, CA; Department of Anatomy, Physiology and Cell Biology, UC Davis School of Veterinary Medicine, CA; Department of Internal Medicine (Hematology), UC Davis School of Medicine, Sacramento, CA; and Veteran Administration Northern California Health Systems, Rancho Cordova, CA.

Submitted July 12, 2001; accepted January 25, 2002.

Supported in part by a University of California Professional Development Award (A.T.W.C.); discretionary gifts to the Biomedical Engineering Division, Department of Medical Pathology, at the University of California Davis Medical

Center (A.T.W.C.); National Institutes of Health grant NIH-R29-HL-55181 (T.W. and A.T.W.C.); and American Heart Association Western States Affiliates grant AHA0050789Y (T.W. and A.T.W.C.).

Reprints: Anthony T. W. Cheung, Dept of Medical Pathology, Research-III Bldg (Rm 3400B), UC Davis Medical Center, 4645 Second Ave, Sacramento, CA 95817; e-mail: atcheung@ucdavis.edu.

The publication costs of this article were defrayed in part by page charge payment. Therefore, and solely to indicate this fact, this article is hereby marked “advertisement” in accordance with 18 U.S.C. section 1734.

© 2002 by The American Society of Hematology

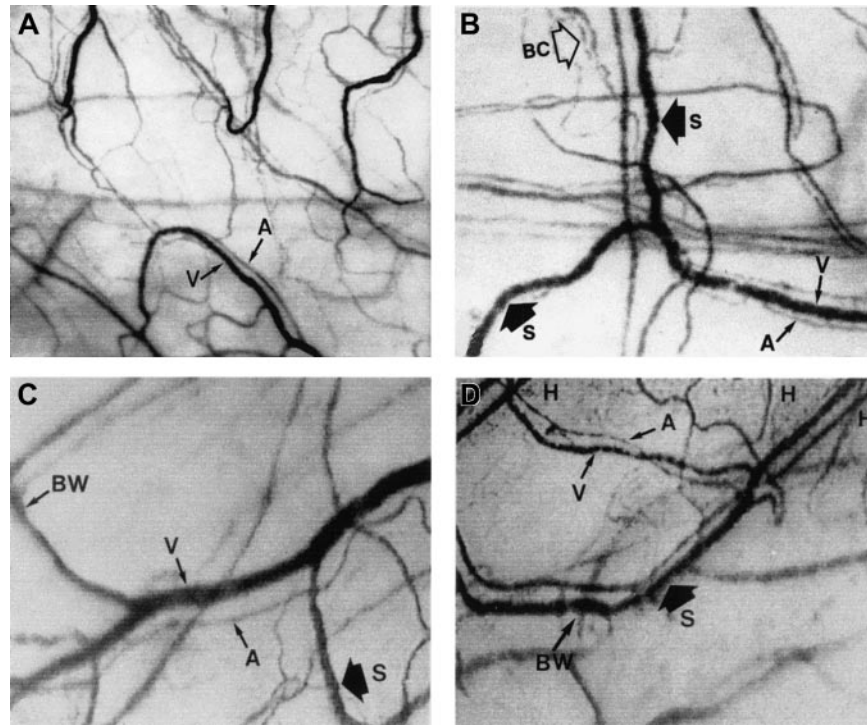


Figure 1. The microcirculation in the bulbar conjunctiva of the eye. Optical magnification, $\times 4.5$; onscreen magnification, $\times 125$. A indicates arteriole; V, venule; H, hemosiderin deposit; S, blood sludging; BW, sacculated vessels (beaded or sausage-shaped); and BC, intermittent boxcar blood flow phenomenon. (A) A typical view of the conjunctival microcirculation of a healthy non-SCD subject to serve as reference (35 mm photograph). Note the even and orderly distribution of the normal-sized arterioles and venules and the normal presence of capillaries. (B) The steady-state conjunctival microcirculation of a patient with nonsevere SCD complications (hard copy of a frame-captured image). All the arterioles and venules in the field are wider in diameter than in non-SCD controls. The bulbar conjunctiva of this SCD patient is adequately vascularized; however, vessel distribution is disorganized and uneven, differing from the healthy non-SCD controls. In addition to blood sludging (S), the overall blood flow is sluggish and intermittent as indicated by the presence of the boxcar blood flow phenomenon (BC) in some vessels. The resolution and clarity of this frame-captured image is comparable to a 35 mm photograph (panel A). (C) The steady-state conjunctival microcirculation of another patient with nonsevere SCD complications (frame-captured image). All the vessels in this image are significantly ($P < .01$) wider in diameter than non-SCD control vessels, and vessel distribution is uneven. Note the unique absence of capillaries and the reduced presence of arterioles and venules in the upper left region of the figure, giving that location a blanched appearance. In addition, sacculated vessels (BW) (beaded or sausage-shaped vessel) and blood sludging (S) are present. (D) The steady-state microcirculation of a patient with severe SCD complications (frame-captured image). Hemosiderin deposits (H) are present, denoting previous extravasation of blood from damaged vessels. The venules are significantly ($P < .01$) wider in diameter than control vessels. In addition, blood sludging (S) and sacculated vessels (BW) are present.

not only for ease of noninvasive access but also for clarity of image display and its uniqueness in being 1 of the 2 accessible microvascular beds in the human body with a complete, true capillary network. Furthermore, the same vessels can be easily identified and relocated for longitudinal investigations. Our laboratory has developed a novel computer-assisted intravital microscopy technology (intravital microscopy coupled with computer-assisted image analysis) to study diabetic microangiopathy and the changes (improvements) in the conjunctival microcirculation after successful simultaneous pancreas-kidney transplantations.²⁰ We have adapted this

noninvasive real-time technology to study and quantify the *in vivo* microvascular abnormalities in SCD.

Patients and methods

Patients and control subjects

SCD patients (ages 16-32 years) were recruited from the Sickle Cell Clinics at the University of California (UC) Davis Medical Center. Eighteen HbSS patients were studied, including 7 with severe and 11 with nonsevere SCD

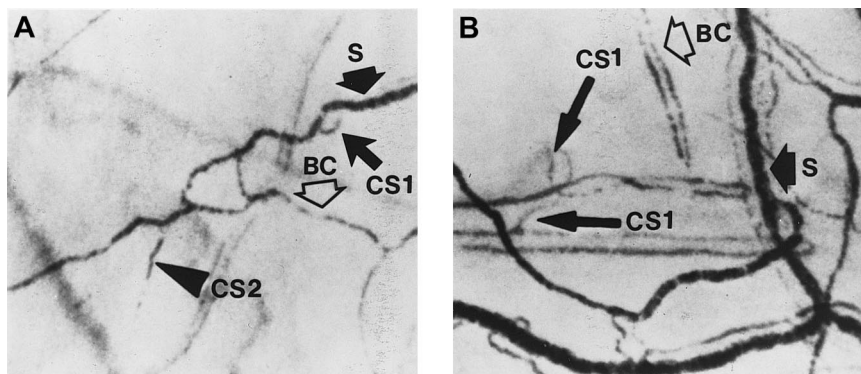


Figure 2. Two frame-captured steady-state images of the conjunctival microcirculation showing additional microvascular abnormalities. Optical magnification, $\times 4.5$; onscreen magnification, $\times 125$. (A) Inadequate vascularization (avascularity), two types of comma signs (CS1 and CS2), and the intermittent boxcar (sluggish) blood flow phenomenon (BC) are present. (B) Another view of comma signs (CS1), blood sludging (S), and the boxcar blood flow phenomenon (BC).

complications. Before we initiated this study, we adopted the following criteria to categorize disease severity:

(1) Patient with severe SCD complications: A patient is considered to have severe SCD complications if he or she has 4 or more hospitalizations for acute painful crisis and/or acute chest syndrome per year or has at least 1 type of soft tissue end organ damage from vasculopathy, including proliferative retinopathy, renal dysfunction (creatinine clearance < 60 mg/mL/min, 24-hour urine protein > 3 g protein per 24 hours, protein-creatinine ratio > 3.5 mg/mg on a spot urine determination), restrictive lung disease (total lung capacity < 70% of predictive values), avascular necrosis, stroke, or nonhealing ulcers.

(2) Patient with nonsevere SCD complications: A patient is considered to have nonsevere SCD complications if he or she has 3 or fewer hospitalizations for acute painful crisis and/or acute chest syndrome per year, along with no soft tissue end organ damage from vasculopathy, proliferative retinopathy, renal dysfunction (creatinine clearance > 60 mg/mL/min, 24-hour urine protein < 3 g protein per 24 hours, protein-creatinine ratio < 3.5 mg/mg on a spot urine determination), restrictive lung disease (total lung capacity > 70% of predictive values), avascular necrosis, stroke, or nonhealing ulcers.

It is recognized that this categorization is arbitrary and that patients identified with “nonsevere” SCD complications by this method could have significant morbidity from the disease. However, this categorization represents an attempt to separate patients broadly to determine if there is any correlation between vasculopathy-induced microvascular abnormalities (based on our *in vivo* technology) and clinical end points (based on medical records).

The painful crisis study was conducted when the SCD patients were hospitalized for crisis treatment. The steady-state study on the same SCD patients was conducted at the time of the patient’s routine (scheduled) monthly visit to the clinic and at the follow-up visit at least 1 month after crisis resolution. Eighteen healthy non-SCD volunteers (ages 15-35 years, with no history of hypertension, diabetes, hyperhomocysteinemia, hypercholesterolemia, hyperlipidemia, chronic renal disease, or cardiovascular disease) were recruited as controls (Table 1). Signed consent was obtained from all SCD patients and non-SCD volunteers (and parents whenever appropriate) before the study. The experimental protocol was approved by the Human Subjects Use Committee at UC Davis and was in accordance with the Declaration of Helsinki.

Computer-assisted intravital microscopy (intravital microscopy coupled with image analysis)

The intravital microscope system was adapted from a prototype originally designed for biomedical engineering research.^{20,21} It has been used successfully to study diabetic microangiopathy in this laboratory²⁰ and has been substantially modified to study *in vivo* microvascular abnormalities in SCD patients.²² The system was macro-optics based and has a fixed optical magnification of $\times 4.5$ at high resolution (equivalent to an onscreen video magnification of $\times 125$). The fixed magnification feature was important because it assured that all steady-state and crisis measurements were made without any magnification variable. The entire optical assembly was securely mounted on a customized stand, and onscreen focusing was performed via a customized focusing platform with orthogonal adjustments. A fiberoptic light source (Fiber-Lite model 3100, Scientific Instrument, Sunnyvale, CA) was fitted with a focusing mechanism to direct a “cool” filtered light beam on the perilimbal region of the bulbar conjunctiva under investigation. A Kodak no. 58 Wratten antired (green) filter was used to enhance the contrast between the conjunctival vessels and the back-

ground. A 35-mm single-lens reflex still camera or a CCD video camera (COHU model 6415-3000, COHU Instrument, San Diego, CA) was attached to the microscope system using a coupling mechanism.

Black-and-white still photographs and videotapes were made on the conjunctival microcirculation by intravital microscopy for subsequent computer-assisted image analysis.²⁰⁻²² The imaging system was PC-based, equipped with an imaging board/frame grabber (Data Translation Model DT2851, Data Translation, La Habra, CA), and was put online with the video system via a FOR-A timer integrator (FOR-A model VTG-33, Scientific Instrument). Video images to be analyzed were frame-captured, coded, digitized, and objectively (blindly) quantified for microvascular characteristics (morphometric or dynamic) using in-house–developed imaging software, VASCAN^{20,21} and VASVEL.²² An area of 8.53 mm² of the conjunctival surface in each frame-captured image was used for computer-assisted data analysis and characterization.²⁰⁻²² The microvascular characteristics studied include vessel morphometry measured by VASCAN²⁰⁻²¹ (using an expansion, nearest neighbor-averaging, local thresholding, and subsequent thinning algorithm) and blood vessel flow dynamics (red cell velocity) measured by VASVEL²² (using a single-step acquisition multiple-frame–tracing algorithm).

Image acquisition—intravital microscopy

The image acquisition protocol was described in detail in previous reports.^{20,22} Briefly, each experimental subject (patient or control) was seated and requested to relax for at least 5 minutes. The subject was also cautioned not to touch or rub the eyes during relaxation. If there was any eye irritation, 2 drops of nonmedicated ophthalmic saline solution were applied and excessive saline was blotted off by tissue at the corner of the eye. The subject again relaxed before videotaping, with the subject’s forehead and chin resting on a head-chin rest and the elbows resting steadily on the bench on which the rest was mounted. The height of the intravital microscope was adjusted to align horizontally with the perilimbal region of the bulbar conjunctiva of the left eye at an angle that provided the flattest surface for focusing. A 35-mm single-lens reflex camera was attached to the system for preliminary focusing and direct visualization of the conjunctival vessels. Antired (Kodak no. 58 Wratten green filter) filtered light was projected and focused on the perilimbal region of the bulbar conjunctiva to enhance image display. With antired epi-illumination, the conjunctival vessels appeared as crisp black lines or tubes on a white background through the viewfinder of the 35-mm camera. Still pictures or slides were taken for reference (Figure 1A). The 35-mm camera was then replaced by the CCD video camera for videotape documentation. During the entire videotaping procedure using intravital microscopy, the images of the conjunctival vessels were viewed and focused onscreen. Normally, a 15- to 20-minute videotape sequence was noninvasively made of each experimental subject, and constant refocusing was conducted to ensure sharp image display. When in focus, the front lens element of the intravital microscope was about 6 cm from the conjunctival surface, and the protocol was designed to obtain a clear view of the perilimbal region of the bulbar conjunctiva without making contact with the eye. Special precaution was taken not to touch the eye or eyelid to prevent physical interference with the microcirculation. Although the vessel images would typically go in and out of focus due to eye movement or blinking, occasional blurred images did not interfere with the study; only 1 captured well-focused video frame was required for each morphometric analysis, and only 8 successive captured frames were needed for each dynamic (red cell velocity) analysis. Selected video images were frame-captured, and hard copies were made via imaging

Table 1. Steady-state hematologic characteristics of the SCD patients

Subjects	Age, y	Hemoglobin, g/dL	Leukocytes, k/mm ³	Platelets, k/mm ³	Reticulocytes, %	F-hemoglobin, %
Patients (from medical record)	35.80 ± 12.07*	8.22 ± 1.31*	12.72 ± 4.18*	323.64 ± 117.66*	10.68 ± 6.19†	31.6 ± 29.5‡
Control range	Adult	12.0-16.0	4.5-13.0	130-400	0.4-2.4	—

*n = 14.

†n = 12.

‡n = 7.

Table 2. Microvascular abnormalities in steady-state SCD

Steady-state microvascular characteristics	Patients with nonsevere SCD complications (n = 11)	Patients with severe SCD complications (n = 7)	Normal controls (n = 18)
Comma signs	2	4	0
Blood sludging	8	7	0
Box car phenomenon	8	7	1
Damaged vessels	2	7	1
Distended vessels	2	7	0
Tortuous vessels	7	7	2*
Sacculated vessels	6	7	0
Microaneurysms	1	4	0

*These 2 controls were contact lens users. A study has shown that the large conjunctival vessels are tortuous around the edge of the contact lens (A.T.W.C., et al, unpublished data, 1996-1997).

technology, with obvious cost, time, convenience, and reliability advantages over 35-mm photography, and with no noticeable loss of image quality (compare Figure 1A with Figures 1B-D, 2, 3, 4). In addition, compensation for image displacement due to eye motion was incorporated into the analytical algorithm for VASVEL.

Different locations (4 to 5) within the perilimbal region of the bulbar conjunctiva of each experimental subject were videotaped to obtain a wide area of coverage. Morphometric and dynamic (red cell velocity) measurements from the various locations were averaged.

For postcrisis return visits or chronological evaluations during crisis resolution, each patient's previous videotape sequence was viewed; features of interest (eg, diameter, ischemic area, avascularity, aneurysm, damaged vessel, or hemosiderin deposit) were identified and relocated for follow-up videotaping (Figure 4). This vessel relocation capability enabled us to restudy or objectively remeasure the same morphometric and dynamic characteristics in various time frames and conditions in longitudinal studies (eg, sequence of events in crisis resolution or an efficacy trial for a medication to test its effectiveness in crisis resolution) and to evaluate intrapersonal measurement variability.

Data analysis

The analytic protocol was described in detail in previous publications.²⁰⁻²² Videotape sequences and images were coded for subsequent analysis to ensure objectivity, with the medical history and identity of the patients blinded to the investigators during analysis. Data analysis was conducted in 2 phases:

(1) Visualization phase—identification of morphometric features. Each videotape sequence was viewed in its entirety. Key landmark morphometric features (characteristics), including comma signs, blood sludging, boxcar blood flow phenomenon, damaged vessels, distended vessels, tortuous vessels, sacculated vessels, and microaneurysms, were identified (Table 2 and Figures 1B-D, 2). The same coded videotape sequence was studied separately by 2 other investigators. Differences in the identification of key features, though extremely infrequent, were discussed and reconciled.

(2) Quantitation phase—computer-assisted image analysis. Four to 5 different video images from each coded videotape sequence were frame-captured for quantitative analysis of vessel morphometry. An area of 8.53 mm² on the bulbar conjunctival surface of each captured frame was used for image analysis. Each selected image was captured, coded, digitized, and quantified using VASCAN^{20,21} to objectively measure average vessel diameter(s) and the total length(s) of arterioles and venules per area for arteriole to venule (A/V) ratio computation (Table 3).

Table 3. Steady-state morphometric measurements of conjunctival vessels in SCD

Experimental subjects	Total length of arterioles per area, cm ⁻¹	Total length of venules per area, cm ⁻¹	A/V ratio	Diameter of venules, μ m		
				Group 1: nonsevere SCD (n = 2)	Group 2: nonsevere SCD (n = 6), severe SCD (n = 6)	Group 3: nonsevere SCD (n = 3), severe SCD (n = 1)
SCD (n = 18)	22.4 \pm 8.7	24.6 \pm 6.3	About 1:1	49 and 52	79 \pm 15	40 \pm 6
Non-SCD controls (n = 18)	26.8 \pm 3.1	49.2 \pm 6.7	About 1:2		55 \pm 4	

Eight successive video images were captured and used for each dynamic measurement of red cell velocity of a selected vessel in the field using VASVEL²² (Table 4). Individual vessel diameter was also measured (using VASVEL) for velocity reference (eg, red cell velocity of 2.9 mm/s in a vessel with a diameter of 78.5 μ m) and for single-vessel correlation with averaged values (using VASCAN).

Statistics

All objective measurements were averaged and reported as mean \pm SD. Variables were compared using analysis of variance. A significance level of .05 was used. *P* values smaller than .01 (eg, .006 844 or 1.13×10^{-7}) were presented as less than .01 for simplicity.

Results

Microvascular characteristics of non-SCD controls

Under intravital microscopy, the conjunctival vessels appeared as well-defined black lines and/or tubes on a white background (Figures 1-4). In the bulbar conjunctiva of the healthy non-SCD control subjects, we observed the orderly presence of an anastomosing network of capillaries, arterioles, and venules without the presence of any ischemic (avascular) zone (Figure 1A); these observations were in agreement with the classic definitive descriptions of Davis and Landau.²³ The normal A/V ratio was about 1:2, and the arterioles and venules exhibited an even microvascular distribution without the presence of dilations, narrowing, microaneurysms, or sacculated vessels. Normal conjunctival blood flow, though variable in red cell velocity, was smooth and consistent (nonintermittent). The ischemic presentation of blood sludging, tortuous or arteriosclerotic vessels, and the boxcar blood flow phenomenon, as previously identified by Davis and Landau for various vascular diseases,²³ was rarely found in the healthy non-SCD (normal) controls. In this study, tortuous vessels were found in 2 non-SCD control subjects; we concluded that this occurrence was caused by contact lens usage and not vasculopathy (A.T.W.C., et al, unpublished data, 1996-1997).

Microvascular characteristics of SCD patients under steady-state conditions

Eighteen SCD patients (7 with severe and 11 with nonsevere SCD complications) were studied. Overall, the conjunctival microcirculation in steady-state SCD differed uniquely from the non-SCD conjunctival microcirculation. The orderly microvascular pattern of the normal bulbar conjunctiva was rarely seen, and abnormal microvascular features were easily recognizable in steady-state SCD patients (Figure 1B-D and Table 2). The A/V ratio was extremely variable and differed significantly (*P* < .01) from the normal non-SCD A/V ratio of about 1:2.

Under steady-state conditions, significant microvascular abnormalities (blood sludging, boxcar blood flow phenomenon, damaged vessels, distended vessels, tortuous vessels, and sacculated vessels) were identified in all 7 patients who had severe SCD complications (Table 2). The presence of comma signs and microaneurysms was identified in only 4 of the 7 patients with severe SCD complications

Table 4. Steady-state conjunctival red cell velocity measurements

Experimental subjects	Close to non-SCD velocity (patients with nonsevere SCD complications, n = 10)	Slower velocity (patients with severe SCD complications, n = 6)	Intermittent trickle flow velocity (patients with nonsevere SCD complications, n = 1; patients with severe SCD complications, n = 1)
SCD (n = 18)	2.0 ± 0.4 mm/s	1.4 ± 0.8 mm/s	< 0.2 mm/s
Non-SCD controls (n = 18)	2.5 ± 0.6 mm/s	—	—

(Table 2). Eleven nonsevere SCD patients, who were relatively free of SCD complications, were found to have fewer manifestations of the above-listed microvascular abnormalities (Table 2). In 2 of the 11 patients with unremarkable SCD history (ie, with nonsevere SCD complications), the steady-state conjunctival microcirculation exhibited a minimal number of microvascular abnormalities, and the microcirculation in these 2 patients was comparable with non-SCD controls.

Morphometric measurements of SCD patients could be separated into 3 groups according to whether the averaged diameter of the conjunctival venules was the same as, significantly wider than, or significantly narrower than the non-SCD diameter (control) range (Table 3). In 2 patients with unremarkable histories of SCD, the averaged diameters of the large vessels (mostly venules) were comparable with non-SCD control values (49 μ m and 52 μ m, respectively; normal control range = 55 ± 4 μ m). Twelve patients had venules with significantly wider diameter (79 ± 15 μ m; $P < .01$) than the controls, with 6 of the 12 patients having severe SCD complications. Four of the remaining patients had venules with narrow diameters (40 ± 6 μ m; $P < .01$) when compared with the controls; 1 of these 4 patients had severe SCD complications. In all 18 patients with SCD, a significant decrease in the presence of capillaries and small arterioles, an abnormal A/V ratio, and uneven vessel distribution were noted when compared with healthy non-SCD controls. In most SCD patients, the microcirculation of the bulbar conjunctiva diminished significantly, resulting in a blanched avascular appearance. At times, the bulbar conjunctiva surface of some SCD patients showed an off-white grayish coloration, with multifocal dark lesions (damaged vessels and/or hemosiderin deposits).

Intrapersonal variability of morphometric measurements in SCD patients under steady-state conditions

Variability of steady-state microvascular features and measurements was minimal in the same patient(s) studied on different days. Intrapersonal variability in steady-state vessel diameter and total length(s) of vessels per area (objectively measured by VASCAN) was 4.1% ± 1.9% and 3.8% ± 2.8%, respectively, in 8 patients (selected at random from the 18 SCD patients) studied on separate steady-state visits scheduled 4 to 12 weeks apart.

Red cell velocity under steady-state conditions

In video sequences showing the conjunctival microcirculation, active blood flow was always visible in some, if not most, conjunctival vessels. However, red cell velocities in different conjunctival vessels varied considerably even in a short video sequence. To ensure this velocity variability was taken into consideration in data interpretation, red cell velocities in at least 5 vessels of each location (measured by VASVEL) were averaged. Then, the averaged red cell velocities of all patients were categorized into 3 red cell velocity groups (Table 4):

(1) Velocity 2.0 ± 0.4 mm/s in 10 patients with nonsevere SCD complications; differed but not significantly from non-SCD control values (2.5 ± 0.6 mm/s).

(2) Velocity 1.4 ± 0.8 mm/s in 6 patients with severe SCD complications; differed significantly ($P < .01$) from non-SCD control values.

(3) Intermittent trickle flow (≤ 0.2 mm/s) in 2 patients; 1 relatively free of SCD (nonsevere) complications and 1 with severe SCD complications. This trickled intermittent red cell movement during steady-state conditions differed significantly ($P < .01$) from steady-state SCD (both group 1 and group 2) and non-SCD control red cell velocities.

Acute and transient microvascular changes during painful crisis

There was a significant decrease in conjunctival vascularity during painful crisis, with a close to complete absence of capillaries and a significantly reduced presence of arterioles and small venules from the steady-state conditions (Figures 3 and 4A). In most cases, the disappearance of capillaries and small arterioles arose as a result of the absence of blood flow into these microvessels.

A few of the sludged large vessels did not show much change in diameter during crisis; however, most of the remaining large vessels showed an averaged decrease of 36.7% ± 5.2% in the diameter (compare Figures 4A and 4B).

Conjunctival red cell velocity, which was measurable in 16 of 18 SCD patients during steady-state conditions (velocity groups 1 and 2 in Table 4), either slowed significantly (46.6% ± 13.1% decrease in red cell velocity from steady-state values; $P < .01$) or was reduced to a trickle (≤ 0.2 mm/s or unmeasurable) when quantified within 5 hours after hospitalization for crisis treatment.

These acute microvascular abnormalities were transient, and the microvasculature reverted to steady-state values after resolution of painful crisis (postcrisis). In reality, normal steady-state values are comparable to postcrisis values made 1 month after crisis resolution. During crisis resolution, reemergence of capillaries and arterioles (reperfusion) was observed in all patients (Figure 4B).

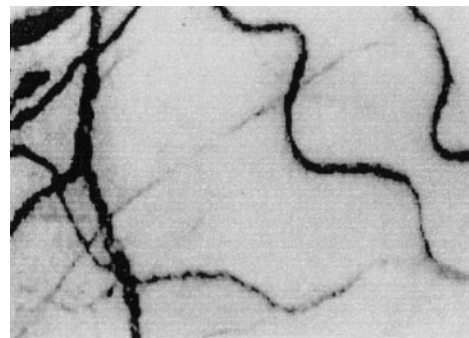


Figure 3. A typical view of the conjunctival microcirculation in an SCD patient 1 hour after hospitalization for painful crisis. Optical magnification, $\times 4.5$; onscreen magnification, $\times 125$. Characteristic landmark features include extreme conjunctival avascularity, complete absence of capillaries, and a further decrease in the presence of arterioles and small venules, giving the bulbar conjunctival surface a more debilitated vascular presentation than the already avascular steady-state blanched appearance. Note the sustained and significant decrease in venular diameter, increased blood sludging caused by the stoppage of blood flow, a sustained and uniform vasoconstriction, and the absence of focal occlusion or constriction in the vessels.

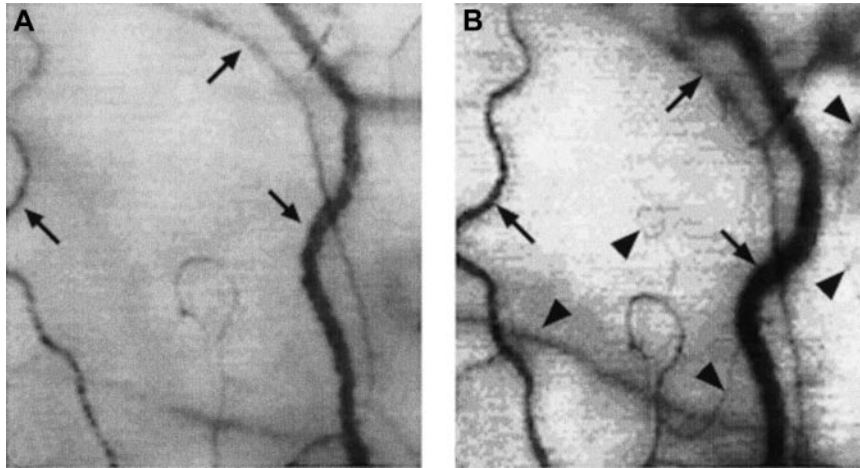


Figure 4. Two frame-captured images showing microvascular changes during crisis resolution in the same SCD patient. Optical magnification, $\times 4.5$; on-screen magnification, $\times 125$. Focusing was aimed at the same location during crisis and crisis resolution, with the same vessel serving as its own reference baseline. (A) During crisis, there is significant reduction in vessel diameter and disappearance of capillaries and arterioles, resulting in extreme avascularity. The arrows point at the three vessels targeted for longitudinal comparison during crisis resolution. (B) An increase in vessel diameter and reappearance of capillaries and arterioles occur during crisis resolution. The vessels indicated by the arrows show a significant increase in vessel diameter. In addition, capillaries and arterioles (arrowheads) reappear during crisis resolution.

Discussion

Using computer-assisted intravital microscopy technology, we have noninvasively identified significant *in vivo* microvascular (morphometric and dynamic) abnormalities in the conjunctival microcirculation of steady-state SCD patients. In this study, blood sludging, the boxcar blood flow phenomenon, damaged vessels, and abnormal vessel density and distribution were consistently present, albeit in varying degrees, in the conjunctival vessels in patients with severe SCD. These observations were significant because the presence of these microvascular abnormalities relates to blood flow impairment and the presence of ischemic zones in the bulbar conjunctiva.¹¹⁻¹⁴ They also correlated with the general concept that vasculopathy normally underlies most of the complications and accounts for much of the morbidity and mortality in SCD.³⁻⁶ The arterioles and venules in some SCD patients were damaged, and hemosiderin deposits were present as multifocal lesions. In addition, vessel tortuosity and microaneurysms were found in some patients. Most of the microvascular abnormalities characterized in this study are in accordance with the classic definitive work of Davis and Landau²³ who first described, via still photography studies, the presence of ischemic zones, blood sludging, boxcar blood flow phenomenon, microaneurysms, tortuous vessels, damaged vessels, and abnormal A/V ratio in vascular diseases. We have observed a unique decrease in overall vascularity, a change in A/V ratio, and abnormal distribution density of vessels in the conjunctival microvasculature under steady-state conditions. The presence of tortuous vessels, blood sludging, and abnormal A/V ratio is indicative of hypoperfusion and ischemia in the bulbar conjunctiva. These *in vivo* pathological conditions have been postulated to exist but have not been directly quantified previously.

The various microvascular abnormalities described above (with the exception of the comma signs and microaneurysms) were found in all 7 patients who were classified as having severe SCD complications and were sporadically found in some, but not all, of the 11 patients with nonsevere SCD complications (Table 2). We speculate that these microvascular abnormalities developed progressively due to tissue remodeling over the course of time and that these abnormal features collectively reflect the severity of the disease state. This study suggests that the sum total of the microvascular abnormalities found in the conjunctival microcirculation correlates with disease severity and clinical outcome of the SCD patients. To facilitate data correlation between disease

severity, microvascular events (steady-state conditions and painful crisis), and hematologic findings, we are currently developing a quantitative Severity Index (computed as a summation of the collective presence of the 15 possible SCD microvascular abnormalities) that can be used by clinicians to assist in the objective evaluation of the clinical course of the disease or to follow disease progression and changes over time and during treatment.

Our work substantially extends earlier observations by other SCD investigators^{6-19,23} and offers several improvements. First, our technology represents the first utilization of a conjunctiva-dedicated intravital microscope design that is not based on the slit-lamp (biomicroscope) assembly previously used in other laboratories.^{6,9-19,23} The magnification and resolution of the optics are better than biomicroscopes, and the system is easy to operate. Coupling the intravital microscope system with videotaping capability offers additional cost, time, convenience, and reliability advantages. In addition, dynamic (red cell velocity) measurements can be conducted on videotapes, an opportunity that did not exist with still photography in historical studies. When combined, these improvements have enabled us to generate detailed and easily reproducible high-resolution images for morphometric and dynamic studies. The computer-assisted capability to frame-capture and objectively quantify (measure) the microvascular characteristics via image analysis further enhances the uniqueness of this technology.

Quantitative and noninvasive studies on blood flow in the *in vivo* human microcirculation have been limited. There are only 2 easily accessible sites for noninvasive *in vivo* microcirculation research in human subjects: the nailfold capillary bed and the conjunctival microcirculation. Lipowsky et al have utilized the nailfold capillaries in the fingers of SCD patients and have commented that the microvascular organization and vessel size in the nailfold microcirculation were not representative of the microcirculation at the organ/tissue level for relevant SCD interpretation.⁷ We used the conjunctival microcirculation because of its easy noninvasive accessibility, excellent quality of image display, and the reliability to relocate the same vessels for longitudinal assessment. In addition, the organizational and morphometric characteristics of the conjunctival microcirculation reflect more closely the characteristics of a true microvascular network (eg, normal presence and distribution of capillaries, arterioles, and venules) and are comparable with those of the microcirculation at the susceptible soft tissue end organ level in SCD.

Under steady-state conditions, 2 putatively healthy SCD patients were shown to have very slow or no blood movement

(intermittent trickle flow) in their conjunctival vessels. This abnormal blood flow pattern differs significantly from normal non-SCD controls and other steady-state SCD patients with measurable blood flow (even in patients with severe SCD complications). One of the 2 patients was relatively free of SCD complications, and the remaining patient had severe SCD complications. Both patients were apparently healthy and not in acute painful crisis. This demonstration of steady-state conjunctival blood flow impairment was unexpected and difficult to explain. We believe that these 2 patients might have inherent cerebrovascular problems^{22,24} and that this conjunctival blood flow impairment might have been triggered by coexisting complications related to SCD. We suspect that abnormalities in large intracranial vessels (eg, middle cerebral artery or internal carotid artery) coexist with abnormalities in small peripheral vessels (eg, conjunctival vessel) in SCD.²² We have also revealed a strong correlation ($P \leq .002$, Fisher exact test) between severely compromised (intermittent trickle flow) conjunctival blood flow with high middle cerebral artery flow velocity (≥ 200 cm/s) and vulnerability to stroke in the same SCD patients in the reported study.²²

This study confirms that computer-assisted intravital microscopy represents the availability of a sensitive, repeatable, and quantitative real-time tool to study microvascular abnormalities in vascular diseases, including SCD. The utilization of the bulbar conjunctiva as a research site provides an ideal, readily accessible, and noninvasive microvascular bed for in vivo research. Moreover, this site offers the additional advantage that the images of the

conjunctival vessels are well resolved and easily identifiable for relocation in longitudinal studies. The fact that the experimental approach is objective and quantitative underscores the uniqueness of this technology and its potential as a clinical and/or research tool. Computer-assisted intravital microscopy (to study small vessel vasculopathy) can be used to correlate with transcranial Doppler ultrasonography or magnetic resonance angiography (to study large vessel vasculopathy) in the prediction of premature stroke in SCD. Intravital microscopy can be used to noninvasively study and identify key in vivo landmark microvascular events in different vascular diseases, including SCD, diabetes, and hypertension. The same objective and quantitative technology can also be used to monitor the efficacy of various therapeutic regimens in SCD, including chronic transfusion, hydroxyurea treatment, and allogeneic bone marrow transplantation. In each case, because the same vessels can be easily identified and relocated for repeated studies, the patient can reliably and appropriately serve as his or her own reference control for longitudinal data interpretation.

Acknowledgment

This manuscript is dedicated to the memory of the late Professor Benjamin Zweifach, a mentor and friend, who was instrumental in initiating 2 of us (A.T.W.C. and P.C.Y.C.) to develop the computer-assisted intravital microscopy technology and to study the conjunctival microcirculation.

References

- Powars D, Chan LD, Schroeder WA. The variable expression of sickle cell disease is genetically determined. *Semin Hematol*. 1990;4:360-376.
- Embury SH, Hebbel RP, Mohandas N, Steinberg MH, eds. *Sickle Cell Disease: Basic Principles and Clinical Practice*. New York, NY: Raven Press; 1994.
- Bunn HF. Pathogenesis and treatment of sickle cell disease. *N Engl J Med*. 1997;337:762-769.
- Platt OS. Easing the suffering caused by sickle cell disease. *N Engl J Med*. 1994;330:783-784.
- Platt OS, Brambilla DJ, Rosse WF, et al. Mortality in sickle cell disease. Life expectancy and risk factors for early death. *N Engl J Med*. 1994;330:1639-1644.
- Francis RB, Johnson CS. Vascular occlusion in sickle cell disease: current concepts and unanswered questions. *Blood*. 1991;77:1405-1414.
- Lipowsky HH, Sheikh NU, Katz DM. Intravital microscopy of capillary hemodynamics in sickle cell anemia. *J Clin Invest*. 1987;80:117-127.
- Rodgers GP, Noguchi CT, Schechter AN. Non-invasive techniques to evaluate the vaso-occlusive manifestations of sickle cell disease. *Am J Pediatr Hematol Oncol*. 1985;7:245-253.
- Rodgers GP, Schechter AN, Noguchi CT, Klein HG, Nienhuis AW, Bonner RF. Microcirculatory adaptations in sickle cell anemia: reactive hyperemia response. *Am J Physiol*. 1990;258:H113-H120.
- Knisely MH, Eliot TS, Warner L. Sludged blood. *Science*. 1947;106:431-435.
- Paton D. The conjunctival sign of sickle cell disease. *Arch Ophthalmol*. 1961;66:90-94.
- Paton D. Conjunctival signs of sickle cell disease. Further observations. *Arch Ophthalmol*. 1962;68:627-632.
- Harding F, Kniseley MH. Setting of sludge in human patients. *Angio*. 1958;9:317-321.
- Fink AJ, Funahashi T, Robinson M, Watson RJ. Conjunctival blood flow in sickle cell disease. *Arch Ophthalmol*. 1961;66:824-829.
- Comer PB, Fred H. Diagnosis of sickle-cell disease by ophthalmologic inspection of the conjunctiva. *N Engl J Med*. 1964;271:544-546.
- Rodgers GP, Schechter AN, Noguchi CT, Klein HG, Nienhuis AW, Bonner RF. Periodic microcirculatory flow in patients with sickle cell disease. *N Engl J Med*. 1984;311:1534-1538.
- Rodgers GP, Roy MS, Noguchi CT, Schechter AN. Is there a role for selective vasodilation in the management of sickle cell disease? *Blood*. 1988;71:597-602.
- Roy MS, Rodgers GP, Podgor MJ, Noguchi CT, Nienhuis AW, Schechter AN. Conjunctival sign in sickle cell anemia: an in-vivo correlate of the extent of red cell heterogeneity. *Br J Ophthalmol*. 1985;69:629-632.
- Serjeant GR, Serjeant BE, Condon PI. The conjunctival sign in sickle cell anemia. A relationship with reversibility of sickle cells. *JAMA*. 1972;219:1428-1431.
- Cheung ATW, Perez RV, Chen PCY. Improvements in diabetic microangiopathy after successful simultaneous pancreas-kidney transplantation: a computer-assisted intravital microscopy study on the conjunctival microcirculation. *Transplantation*. 1999;68:927-932.
- Chen PCY, Kovalcheck SW, Zweifach BW. Analysis of microvascular network in bulbar conjunctiva by image processing. *Int J Microcirc Clin Exp*. 1987;6:245-255.
- Cheung ATW, Harmatz P, Wun T, et al. Correlation of abnormal intracranial vessel velocity (measured by transcranial Doppler ultrasonography) with abnormal conjunctival vessel velocity (measured by computer-assisted intravital microscopy) in sickle cell disease. *Blood*. 2001;97:3401-3404.
- Davis E, Landau J. *Clinical Capillary Microscopy*. Springfield, IL: Charles C Thomas; 1966.
- Adams R, McKie V, Nichols F, et al. The use of transcranial ultrasonography to predict stroke in sickle cell disease. *N Engl J Med*. 1992;326:605-610.